Polymer Journal (2017) 49, 625–632

www.nature.com/pj

ORIGINAL ARTICLE

Structure and properties of biocompatible poly(glycerol adipate) elastomers modified with ethylene glycol

Lucila Navarro[1], Natalia Ceaglio[2] and Ignacio Rintoul[1]

Polyesters poly(glycerol adipate)s or PGAs were prepared through a catalyst-free polycondensation reaction involving different proportions of adipic acid and glycerol. Additionally, another set of PGAs was formulated by adding ethylene glycol to the reaction mixture, creating three PGA-*co*-ethylene glycols of different ethylene glycol-to-glycerol ratios. All prepolymers were chemically crosslinked into elastomeric films according to specific experimental conditions. A full characterization of elastomers revealed an ease of tunability according to monomer ratios and curing conditions. Mechanical properties presented a variety of Young's modulus values ranging from 0.07 to 8.33 MPa. Within this range, a number of Young's modulus values of soft tissues can be included. Moreover, a cytotoxicity analysis performed on embryonic mouse fibroblasts (NIH/3T3) showed an absence of cytotoxicity and good adherence over all PGA and PGA-*co*-ethylene glycol elastomers. In addition, fibroblasts underwent a differentiation process into neuron-like cells, thus exhibiting excellent potential for soft tissue engineering.
Polymer Journal (2017) **49,** 625–632; doi:10.1038/pj.2017.30; published online 21 June 2017

INTRODUCTION

Over recent decades, the study of synthetic biomaterials has emerged as an important field of research owing to a need for novel materials for therapeutic applications such as tissue engineering systems, platforms for drug delivery, coatings of biomedical prosthesis and implants to increase biotolerability levels. The most commonly used biodegradable materials are aliphatic polyesters, especially poly(lactic-*co*-glycolic acid) and poly(lactic acid). However, the use of these polymeric materials present severe limitations (i.e., rigid mechanical properties, undesirable bulk degradation patterns and excessive water uptake), resulting in extreme deformation during degradation.[1,2] In this context, elastomeric polymers have emerged as an interesting alternative given that their flexible properties render them suitable for soft tissue applications such as blood vessels, heart valves, cartilage and tendons.[3–6] In addition, as surface-eroding polymers, slight deformations are detected upon degradation in combination with linear mass and progressive strength loss.[2,3,7]

Although several biodegradable elastomers have been developed,[8–10] most are obtained through complex and demanding synthetic procedures, which translates into high manufacturing costs, thus limiting their commercial and clinical use.[11] Of the various innovative polyesters that have recently been reported, poly(glycerol-adipate) or PGA appears to be a promising material because of its versatility and simplicity. It is noteworthy that both monomers, glycerol and adipic acid, required for PGA synthesis have been approved by the Food Drug Administration as safe materials.[12] Thus, Zhang *et al.*[12,13] have obtained hyperbranched PGA polyesters and have focused their attention on structural analyses and thermal properties.[12,13] The experimental procedure reported for the preparation of hyperbranched polymers involves a polycondensation reaction of glycerol and adipic acid using dibutyltin oxide as a catalyst.[12] A variation of the synthesis involves the use of a lipase–esterase to promote a reaction between divinyl adipate and glycerol, generating low-molecular-weight polymers.[14,15]

Despite the countless applications of PGA used in the biomedical field, only the use of PGA as a hyperbranched polymer has been reported, and therefore, the present work will specifically focus on crosslinked elastomeric films developed through thermal curing. To do so, we have developed a catalyst-free synthesis of PGA prepolymers that can then be converted to the required elastomer through crosslinking under specific thermal conditions. Different amounts of ethylene glycol were used as comonomers in polymerization reactions, affording elastomers with tunable properties that may be suited for soft tissue engineering applications. The polymers were fully characterized via standard spectroscopic methods. Thermal and mechanical properties of the resulting elastomeric films were evaluated. In addition, hydration and degradation behaviors were analyzed, and cytotoxicity assays were performed on embryonic mouse fibroblasts.

EXPERIMENTAL PROCEDURES

Materials

Adipic acid, deuterated chloroform chloroform-d ($CDCl_3$), dimethylsulfoxide (DMSO) and tetrahydrofuran were obtained from Sigma-Aldrich (St Louis,

[1]Instituto de Desarrollo Tecnológico para la Industria Química (INTEC), Consejo Nacional de Investigaciones Científicas y Técnicas (CONICET), Universidad Nacional del Litoral (UNL), Santa Fe, Argentina and [2]Laboratorio de Cultivos Celulares, Facultad de Bioquímica y Ciencias Biológicas, Consejo Nacional de Investigaciones Científicas y Técnicas (CONICET), Edificio FBCB-Ciudad Universitaria UNL, Universidad Nacional del Litoral (UNL), Santa Fe, Argentina
Correspondence: Dr L Navarro, Instituto de Desarrollo Tecnológico para la Industria Química (INTEC), Consejo Nacional de Investigaciones Científicas y Técnicas (CONICET), Universidad Nacional del Litoral (UNL). Colectora Ruta Nac 168, Paraje El Pozo, Santa Fe 3000, Argentina.
E-mail: lucila.navarro12@gmail.com
Received 3 January 2017; revised 25 April 2017; accepted 11 May 2017; published online 21 June 2017

Table 1 Synthesis and properties of PGA prepolymers 1a and b and PGA-*co*-ethylene glycol prepolymers 2a–c

Entry	*Prepolymer*[a]	*Mn*	*Mw*	*PDI*	*DB (%)*	*AA/G/EG*[b]	*AA/G/EG (NMR)*[c]	*Yield (%)*[d]
1	**1a**	2050	4500	2.2	40.5	1/1	1/0.98	77.2
2	**1b**[e]	1700	12 500	7.3	60.0	1/0.6	1/0.65	117.9
3	**2a**	2200	5700	2.6	44.0	1/0.75/0.25	1/0.79/0.24	80.2
4	**2b**	1980	5400	2.7	41.1	1/0.50/0.50	1/0.55/0.45	72.2
5	**2c**	1680	4900	2.9	27.5	1/0.25/0.75	1/0.3/0.69	68.2

Abbreviations: AA: adipic acid; $CDCl_3$: deuterated chloroform; DMSO: dimethylsulfoxide; EG: ethylene glycol; G: glycerol; ^{1}H-NMR: proton nuclear magnetic resonance; Mn: number-average molecular weight; Mw: weight-average molecular weight; PDI: polydispersity index.
[a]Reaction conditions: 17 h at 150 °C, then 4 h at 150 °C under vacuum.
[b]Molar ratio of AA, G and EG.
[c]Determined by ^{1}H-NMR in $CDCl_3$ containing 5% DMSO.
[d]Determined by mass loss method.
[e]Reaction conditions: 16 h at 150 °C, then 0.5 h at 150 °C under vacuum.

MO, USA). Glycerol (99%) and ethylene glycol were purchased from AppliChem/BioChemica (Darmstadt, Germany). Poly(lactic-*co*-glycolic) acid (80:20 lactic/glycolic ratio) with a viscosity of 1.7–2.6 dl g^{-1} was obtained from Resomer. All reagents were used as received unless stated otherwise.

Prepolymer synthesis and characterization

The synthesis of PGA was performed as follows: 5.52 g of glycerol (60 mmol) and 8.76 g of adipic acid (60 mmol) were added to a round-bottom flask equipped with a Dean Stark trap and a reflux condenser. The reaction mixture was constantly stirred while being subject to a temperature of 150 °C in an N_2 atmosphere for 17 h. Then, the reaction mixture was heated for 4 h at the same temperature under high vacuum (3 mm Hg) and was allowed to reach room temperature. The COOH/OH ratio was varied by adjusting the monomer proportions (Table 1). PGA-modified prepolymers were obtained by adding specific amounts of ethylene glycol to the bulk mixture. Three different PGA–ethylene glycol polymers were obtained (Table 1).

Gel permeation chromatography analyses were performed with a Waters 1525 instrument equipped with a refractive index detector (Waters 2414) and a Waters Styragel HR4+HR1 column. Prepolymer solutions (1 wt%) were prepared in tetrahydrofuran. The elution rate was 1 ml min^{-1} (tetrahydrofuran) and polystyrene standards were used for the molecular weight calibration curve.

Proton nuclear magnetic resonance (^{1}H-NMR) spectra (300 MHz) were obtained with a Bruker Avance II spectrometer (Karlsruhe, Germany) using $CDCl_3$ and 5% DMSO as a cosolvent and were referenced to residual solvent signals.

The branching degree (BD%) was calculated based on NMR spectra.[16] Specific peak signals from 1,2,3-triacylglyceride (D), 1,2-diacylglyceride ($L_{1,2}$) and 1,3-diacylglyceride ($L_{1,3}$) were used for BD% calculations according to Equation (1):

$$\mathrm{BD}\% = \frac{2D}{2D + (L_{1,2} + L_{1,3})} \times 100 \quad (1)$$

Fourier transform infrared spectra were obtained with a Shimadzu 8201 PC apparatus (Kyoto, Japan).

Yields of the esterification reactions were determined by weighting the reaction mixture before and after synthesis reactions. Weight loss occurring during the polycondensation reaction was assumed to be due to water removal. The amount of dicarboxylic acid converted to esters was calculated according to Equations (2) and (3):

$$\text{Reaction yield } (\%) = \frac{\text{moles of reacted carboxylic group}}{\text{moles of original carboxylic group}} \times 100 \quad (2)$$

$$\text{Reaction yield } (\%) = \frac{m_{H_2O}/M_{H_2O}}{2 \times m_{AA}/M_{AA}} \times 100 \quad (3)$$

where m_{H_2O} is the mass of water eliminated upon reaction and M_{H_2O} is the molecular weight of water, m_{AA} is the mass of adipic acid used in the synthesis and M_{AA} is the molecular weight of adipic acid.

Film preparation and characterization

All prepolymers were dissolved in tetrahydrofuran, and the solutions were cast onto glass slides previously treated with a thin layer of alginate. The solvent was allowed to evaporate at room temperature overnight, and then slides were heated in an oven for curing at 120 °C for 3 and 5 days. After cooling, the glass slides were placed in water to delaminate the elastomeric films.

A postcuring treatment was performed to eliminate unreacted monomers. The films were placed in increasing concentrations of ethanol–water solution (50%, 60%, 80% and 100% ethanol, respectively) for 2 h each.

Gel content levels were determined using a Soxhlet extraction system. Boiling ethanol was used as the extraction solvent. Samples were left for 24 h and were allowed to dry at room temperature. Films were weighed before and after the test. Gel content levels were obtained from Equation (4):

$$\text{Gel content } (\%) = \frac{m_f}{m_i} \times 100 \quad (4)$$

where m_i and m_f are the initial and final mass of elastomeric film, respectively.

Static contact angle measurements were performed with a goniometric OCA 20 device (Dataphysics, San Jose, CA, USA). Static contact angle values were determined using the sessile drop method and using distilled water as dispensed liquid. The Young–Laplace procedure was used as a processing method. Five static contact angle measurements were performed per polymer film.

Swelling indexes by hydration were performed by immersing the elastomeric samples (8 mm in diameter and 1 mm thick) in a phosphate-buffered saline (PBS) buffer solution of pH 7.4. The samples were withdrawn at different times, and the excess of water was carefully removed from the surface and then weighed. The swelling index was calculated according to Equation (5):

$$\text{Swelling index } (\%) = \frac{W_s - W_o}{W_o} \times 100 \quad (5)$$

where W_s is the wet mass and W_o is the initial dry mass.

Thermal gravimetric analyses (Mettler-Toledo TGA/SDTA851e/LF/1100; Mettler-Toledo, Colombus, OH, USA) were performed in air at room temperature to 750 °C at a heating rate of 10 °C min^{-1}. Differential scanning calorimetry (Mettler-Toledo 821) scans were performed by heating and cooling rates of 10 °C min^{-1} at intervals of − 50 °C to 150 °C under nitrogen.

For tensile properties, dog bone-shaped specimens were cut from the polymeric films for mechanical testing. Tensile assays were performed at room temperature with an Instron 3344 universal testing machine (Norwood, MA, USA) equipped with a 100 N load cell. The elongation rates were maintained at 10 mm min^{-1} and all samples were elongated to failure. The Young's modulus (YM) was calculated from the initial slope of the stress–strain curves of three samples.

Crosslinking densities (n) were estimated based on the theory of rubber elasticity using Equation (6):

$$n = \frac{\mathrm{YM}}{3RT} \quad (6)$$

where n is the number of network chain segments per unit volume (mol m^{-3}), Young's modulus is the Young's modulus (Pa), R is the universal gas constant level (8.3144 J $mol{\cdot}K^{-1}$) and T is the absolute temperature (295 K).

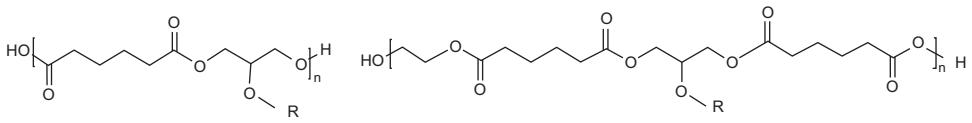

1a-b **2a-c**

Figure 1 Schematic chemical structure of PGA (**1a** and **b**) and PGA-*co*-ethylene glycol (**2a–c**). R is H or the polymer chain.

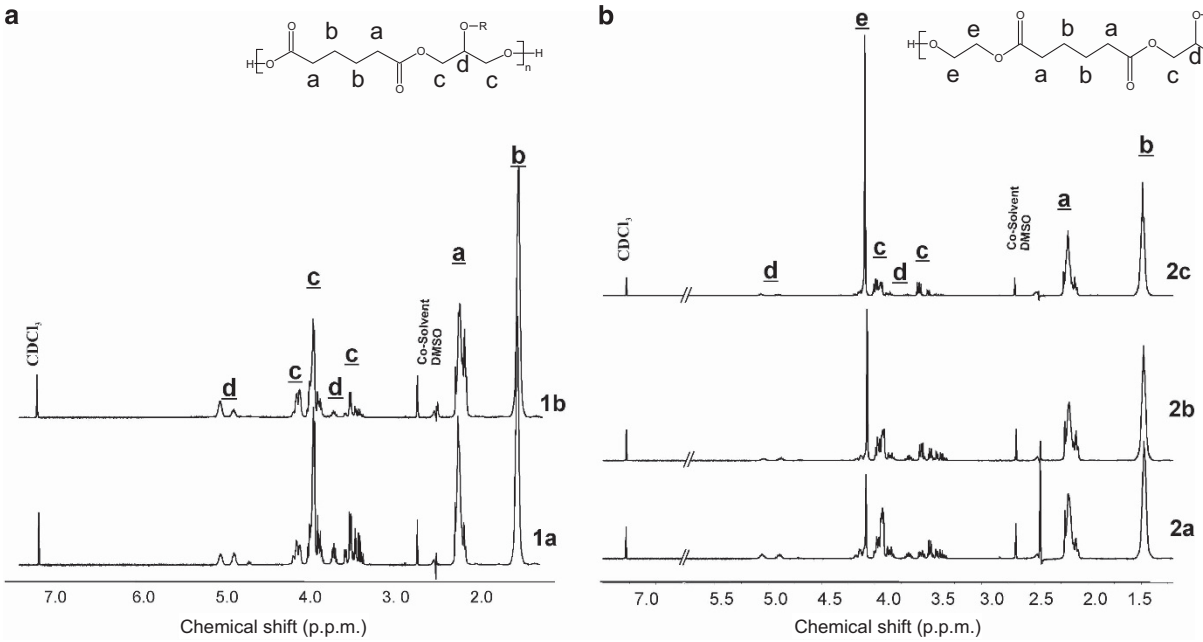

Figure 2 Proton nuclear magnetic resonance (^{1}H-NMR) spectra of prepolymers (**a**) **1a** and **b** and (**b**) **2a–c**.

In vitro degradation studies were performed in PBS buffer (pH 7.4) at 37 °C. Disk-type cured polymer samples (8 mm in diameter and 1 mm thick) were immersed in PBS buffer for predetermined periods of time, after which the samples were withdrawn from the immersion medium, washed with deionized water and left to dry for 48 h at 50 °C for final weight measurements. Mass losses were calculated from the dry mass at point p (M_p) and from the initial dry mass (M_o) of the sample according to Equation (7).

$$\text{mass loss } (\%) = \frac{(M_o - M_p)}{M_o} \times 100 \qquad (7)$$

In vitro cell attachment, proliferation and cytotoxicity

NIH/3T3 embryonic mouse fibroblasts (ATCC CRL-1658) were used as model cells for *in vitro* adhesion, proliferation and cytotoxicity evaluation. Cells were grown in Dulbecco's modified Eagle's medium (Gibco, Waltham, MA, USA) supplemented with 10% fetal calf serum (Gibco) and 2 mM L-glutamine (Gibco) at 37 °C in a humidified atmosphere at 95% in air and at 5% in CO_2. Elastomeric films were prepared as described above at 120 °C for 5 days. All polymers were cut into 5 mm discs and sterilized through a treatment with 70% ethanol. Polymer discs were placed in 96-well plates, were air-dried for 24 h under sterile conditions and were exposed to UV light for 15 min. NIH/3T3 cells were trypsinized and seeded in 96-well plates at densities of 2500 and 5000 cells per well (for proliferation evaluation) or 20 000 cells per well (for cytotoxicity assessment) in the presence or absence of polymer discs. Cell attachment and morphology patterns were monitored by microscope observation and photography at different time points. Proliferation was assessed from the MTS assay using a Chromogenic Kit (CellTiter 96 AQueous Non-Radioactive Cell Proliferation Assay; Promega, Madison, WI, USA) after 48 h of culturing. The plates were inspected at 492 and 690 nm with a microplate reader and the signal intensity was reported as the mean of the absorbance measured in four wells. For cytotoxicity evaluations, cells were harvested by trypsinization, stained with 0.4% trypan blue (Sigma) and counted using a hemacytometer. The results were statistically analyzed through one-way analysis of variance, followed by a Tukey's multiple comparison test.

RESULTS AND DISCUSSION

Synthesis and characterization of prepolymers

PGA **1** and PGA-*co*-ethylene glycol **2** were obtained by bulk polycondensation at 150 °C (17 h), followed by reactions conducted at a reduced pressure level (4 h, 150 °C). A schematic representation of the chemical structures is shown in Figure 1. Monomer ratios were varied to achieve different crosslinking degrees and final elastomeric properties. The specific monomer ratio together with number-average molecular weight (Mn), weight-average molecular weight (Mw) and polydispersity index values for the prepolymers are shown in Table 1 (entries 1–5). All prepolymers were obtained as yellowish viscous liquids. The highest Mw and polydispersity index values were obtained for PGA **1b** (60 mol% of glycerol, entry 2 in Table 1). This result is not surprising given that the **1b** preparation involved the lowest amount of trifunctional hydroxyl compound, causing the entanglement state to be reached sooner than was the case for the other prepolymers. This is also supported by the BD% parameters, which presented the highest value of all of the evaluated prepolymers as is shown in Table 1. To curtail undesirable premature crosslinking effects, the reaction time under vacuum conditions should be reduced to 0.5 h (entry 2 in Table 1).

Esterification yields were calculated using the mass loss method. For all of the prepolymers with the exception of **1b**, esterification levels

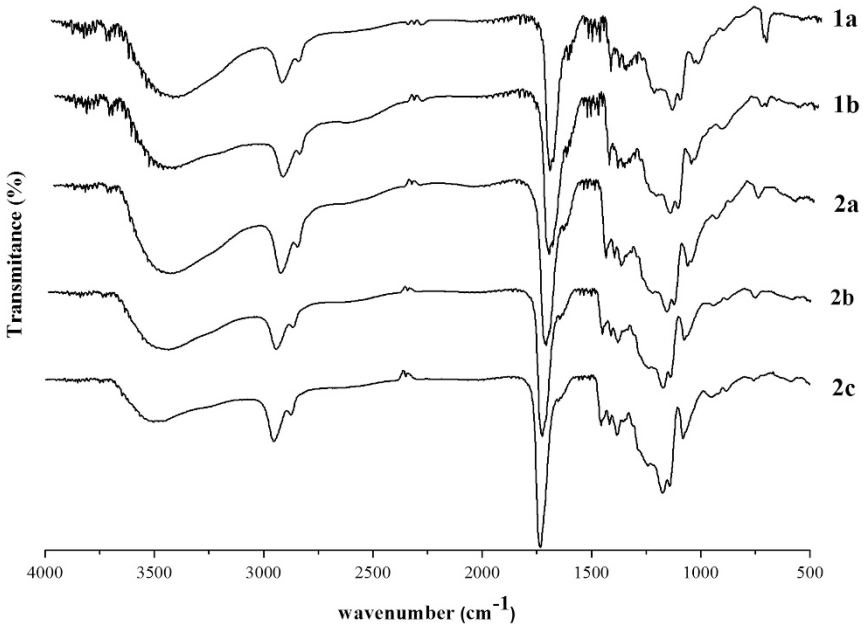

Figure 3 Fourier transform infrared (FT-IR) spectra of prepolymers **1a** and **b** and **2a–c**.

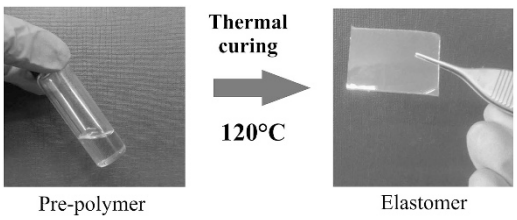

Figure 4 Photos of the prepolymer and elastomeric film resulting from the thermal treatment.

ranged between 70 and 80% (entries 1 and 3–5, Table 1). For prepolymer **1b**, an esterification yield of higher than 100% was obtained. This unexpected result is attributed to the occurrence of glycerol evaporation during the condensation reaction. This result was confirmed through its detection from eliminated water after vacuum treatment by gas chromatography coupled to a flame ionization detector (Agilent Technologies, Santa Clara, CA, USA; 6890N Network GC System). On this issue, Li *et al.*[7] compared mass loss and titration trends via the potassium hydroxide method during poly (glycerol sebacate) preparation and found negligible glycerol elimination patterns within the first 24 h of reaction at 130 °C, showing that the mass loss method supports a worthy approximation of esterification yields during the first stage of reaction.

Prepolymers were dissolved in $CDCl_3$ containing 5% DMSO for ^{1}H-NMR analyses. DMSO-d_6 is not used as a solvent in ^{1}H-NMR studies, as residual water signals, which appear at 3.33 p.p.m., would overlap with the expected peaks of prepolymers **1** and **2**. Thus, we found that 5% DMSO in $CDCl_3$ was sufficient to completely dissolve the prepolymers while still leaving the region of ~3.3 p.p.m. free. After proving that DMSO did not overlap with prepolymer signals, ^{1}H-NMR spectra were obtained using a Bruker WATERSUP pulse sequence (Karlsruhe, Germany) with an o1p of 2.50 p.p.m. to diminish the cosolvent signal intensity level. ^{1}H-NMRs of prepolymers **1a** and **b** and **2a–c** are shown in Figures 2a and b, respectively. ^{1}H-NMR spectra of **1a** and **b** (Figure 2a) show expected signals in the region of 1.4–2.2 p.p.m. belonging to adipic acid CH_2 aliphatic chains. Signals corresponding to deshielded CH_2 and CH protons of di- and triacyl glycerol appear at between 3.0 and 4.5 and 4.5 and 5.5 p.p.m., respectively. ^{1}H-NMR values of **2a–c** (Figure 2b) also show an intense peak at ~4.0 p.p.m. that is assigned to the CH_2 of the ethylene glycol units. As was expected, the highest intensity peak at 4.0 p.p.m. was obtained for prepolymer **2c**, which has the highest ethylene glycol content.

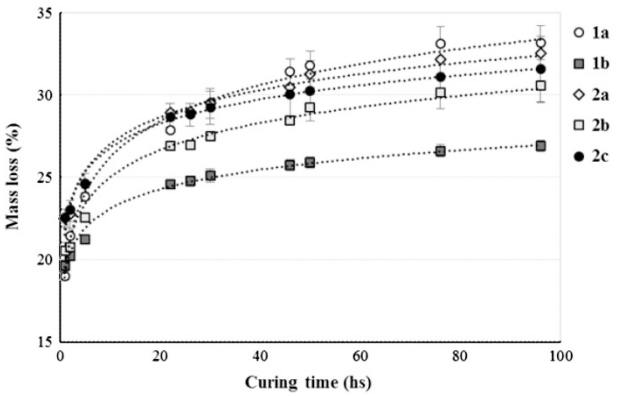

Figure 5 Mass loss with curing time. Time zero represents the mass loss obtained from each prepolymer synthesis.

Infrared spectra of prepolymers **1a** and **b** and **2a–c** are shown in Figure 3. All spectra show a sharp and strong peak at 1750 cm^{-1} corresponding to carboxylic C=O stretching. Furthermore, typical aliphatic C–H absorption peaks appear at 2670 cm^{-1} and O–H stretching is observed as a broad peak at ~3500 cm^{-1}.

Elastomeric film characterization

All prepolymers were crosslinked (i.e., cured) by thermal treatment to obtain elastomeric films as shown in Figure 4.

Mass loss curves for the curing process are shown in Figure 5. Time zero represents the mass loss obtained after each prepolymer synthesis.

For all of the polymers, mass loss grows logarithmically with curing time and mainly due to the formation of new ester bonds and water release. As was expected, polymer **1b** presents the lowest levels of mass loss over the curing period, as it has the lowest glycerol content and a smaller ratio of alcohol and acidic groups than the rest of the polymers. No significant difference was observed for PGA-*co*-ethylene glycol elastomers **2a–c**.

As shown in Table 2, the thermal decomosition temperature (T_d) obtained from the thermal gravimetric analyses was ~400 °C for all of the elastomers. In addition, differential scanning calorimetry scans shown in Figure 6 illustrate that all of the elastomers occupy a rubbery state at 37 °C. Glass transition temperature (T_g) values increase as the OH/COOH ratio decreases for polymers **1a** and **b** (Figure 6a). Thus, elastomer **1b** presents a T_g 10 °C value that is higher than that of **1a**, which has higher levels of glycerol content. The T_g value decreases as ethylene glycol content increases for polymers **2a–c** (Figure 6b), registering values of −20, −24.5 and −30 °C for **2a**, **2b** and **2c**, respectively.

Gel content analysis can be used to estimate curing process efficiency levels. When polymers are placed in boiling ethanol, unreacted materials diffuse from the elastomeric network into the medium, resulting in mass loss. As shown in Table 2, gel content levels

Table 2 General properties of elastomeric films

Elastomer	T_d *(°C)*	T_g *(°C)*	*GC3 (%)*	*GC5 (%)*	*SW (%)*	*CA (deg.)*
1a	400	−15	98.9±0.3	99.0±0.2	10.8±0.2	70.2±4.9
1b	398	−2.5	98.7±0.3	99.6±0.2	10.7±0.1	80.2±3.4
2a	398	−20	98.5±1.2	99.0±0.5	13.3±0.2	75.8±3.6
2b	396	−24.5	95.2±3.2	98.1±3.2	8.1±0.6	80.5±4.4
2c	401	−30	85.0±5.2	92.2±3.3	6.7±0.3	89.0±3.6

Abbreviations: CA: contact angle; GC3: gel content after 3 days of curing; GC5: gel content after 5 days of curing; SW: swelling; T_g: glass transition temperature; T_d: thermal decomposition temperature.

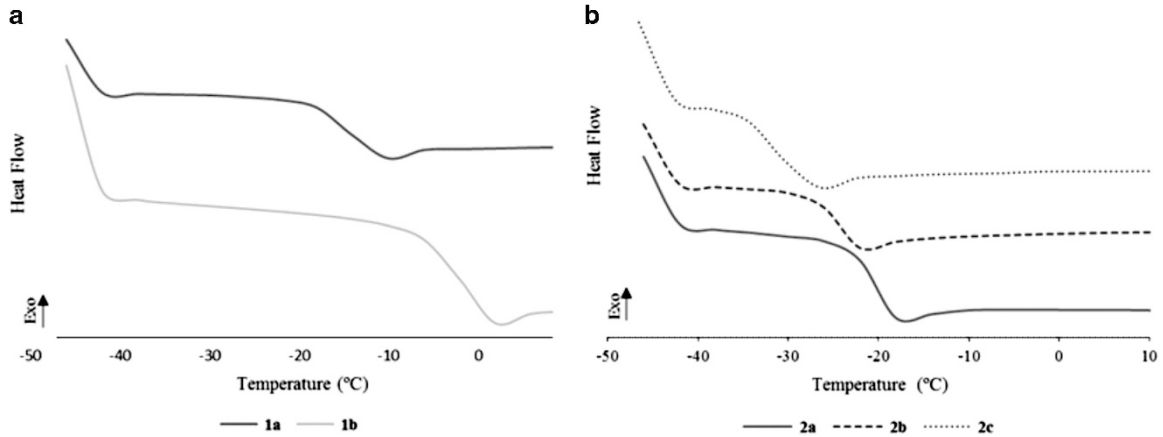

Figure 6 Differential scanning calorimetry (DSC) analysis of elastomers: (**a**) **1a** and **b** and (**b**) **2a–c.**

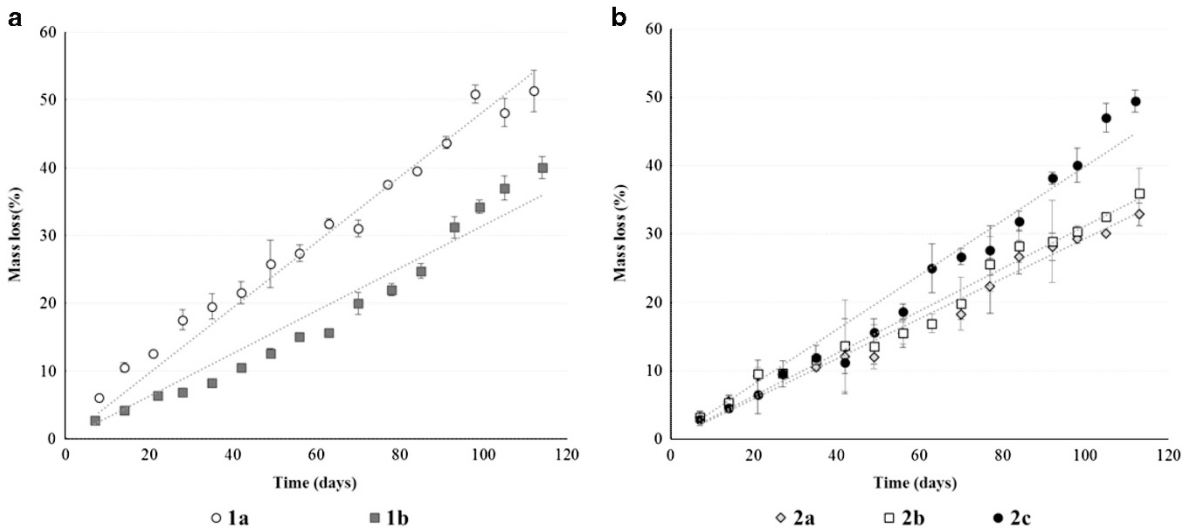

Figure 7 *In vitro* degradation profiles of elastomers: (**a**) **1a** and **b** and (**b**) **2a–c.**

tend to increase with curing time. After 5 days of curing, all elastomers presented gel content values higher than 98%, with the exception of **2c**, which reached an acceptable value of 90%. A clear trend in gel content values can be observed for PGA-*co*-ethylene glycol polymers **2a–c**. Elastomers with lower levels of glycerol require more time to achieve an elastomeric network with low monomer residuals, showing lower values of gel content under the same curing conditions.

It is well known that the hydrophilicity, hydration abilities and degradation profiles of biomaterials have a key role in their behavior when placed in the body. Hence, water contact angles were measured for all of the elastomers and corresponding results are presented in Table 2. Contact angle values of **1a** and **b** and **2a–c** were lower than 90°. During curing, OH groups from glycerol and ethylene glycol reacted with COOH groups of adipic acid units, creating new ester linkages. Thus, polar and protic COOH groups would no longer be available to interact with water from the aqueous medium, producing contact angles of $<90°$. We also found that as the glycerol content of **2a–c** decreases, the contact angle increases. This lower level of glycerol translates into a lower content of hydrophilic OH groups located along the surface of the elastomer, leading to the generation of more hydrophobic polymers.

The hydration properties of elastomers were further evaluated from the equilibrium water content after immersing the samples in PBS (pH 7.4) (Table 2). All swelling indexes reached a plateau within the first 24 h of immersion, representing the maximum degree of water uptake registered over the 30 days of study. Although a significant

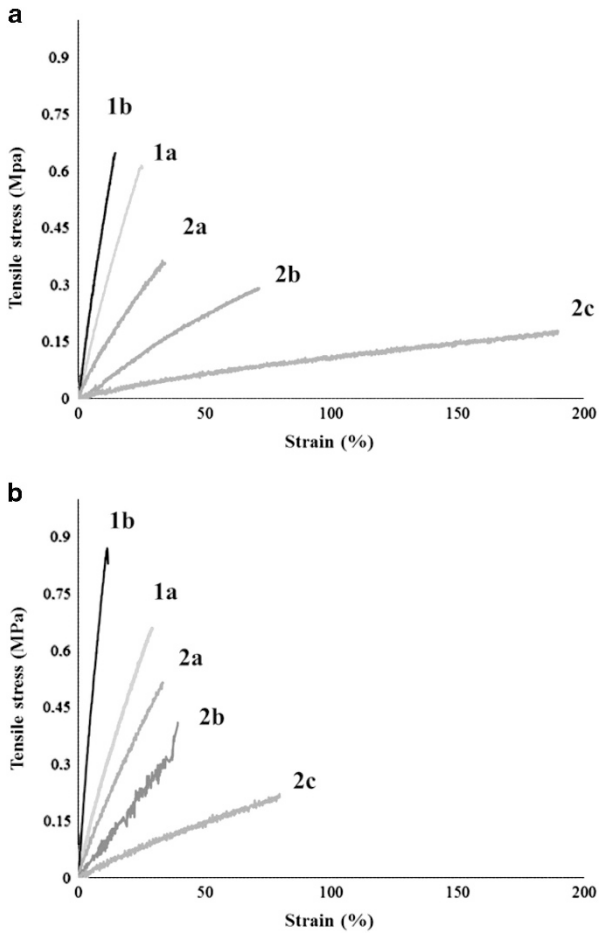

Figure 8 Stress–strain curves of elastomers from representative experiments ($n=3$). (**a**) Three-day-cured elastomers and (**b**) 5-day-cured elastomers.

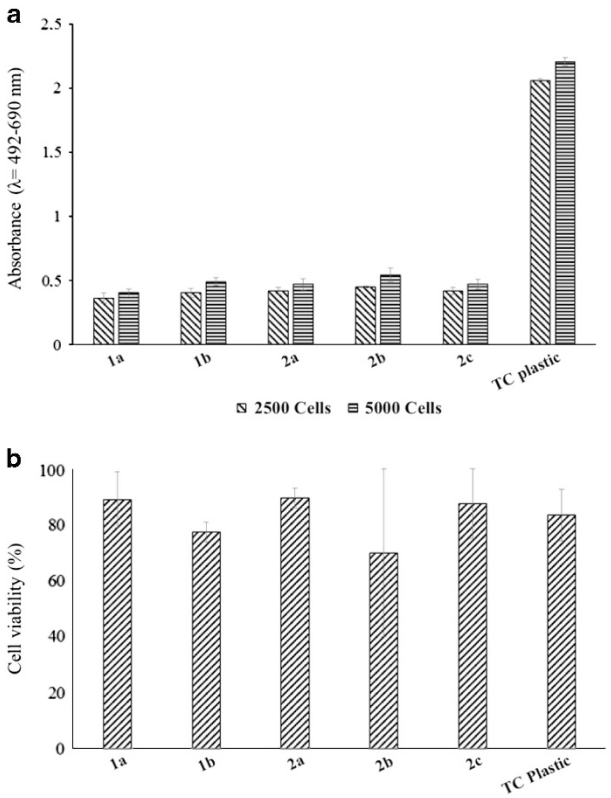

Figure 9 (**a**) *In vitro* cell proliferation of NIH/3T3 fibroblasts on elastomers **1a** and **b** and **2a–c**; 2500 and 5000 cell seeding after 48 h. (**b**) Cytotoxicity evaluation of polymers **1a** and **b** and **2a–c** on NIH/3T3 cells; 20 000 cell seeding after 48 h.

Table 3 Mechanical properties of elastomeric films cured for 3 and 5 days

Elastomer	*3 days cured*				*5 days cured*			
	YM (MPa)	*UT (MPa)*	*UD (%)*	*$n\times10^{-4}$ (moles cm^{-3})*	*YM (MPa)*	*UT (MPa)*	*UD (%)*	*$n\times10^{-4}$ (moles cm^{-3})*
1a	2.41±0.09	0.4±0.19	28.5±2.1	3.28±0.12	3.11±0.8	0.60±0.06	26.2±3.9	4.2±0.4
1b	5.00±0.72	0.68±0.06	14.73±0.09	6.8±0.98	8.33±1.42	0.85±0.24	7.7±2.6	11.4±1.9
2a	1.18±0.18	0.35±0.05	30.1±7.0	1.61±0.25	1.50±0.10	0.43±0.11	28.7±6.7	2.0±0.1
2b	0.43±0.01	0.25±0.07	75.5±2.9	0.59±0.09	0.89±0.45	0.35±0.09	40.1±5.2	1.2±0.09
2c	0.07±0.02	0.16±0.06	193.8±6.1	0.09±0.03	0.23±0.33	0.21±0.03	86.9±6.8	0.30±0.04

Abbreviations: n: crosslinking degree; UD: ultimate deformation; UT: ultimate tension; YM: Young's modulus.

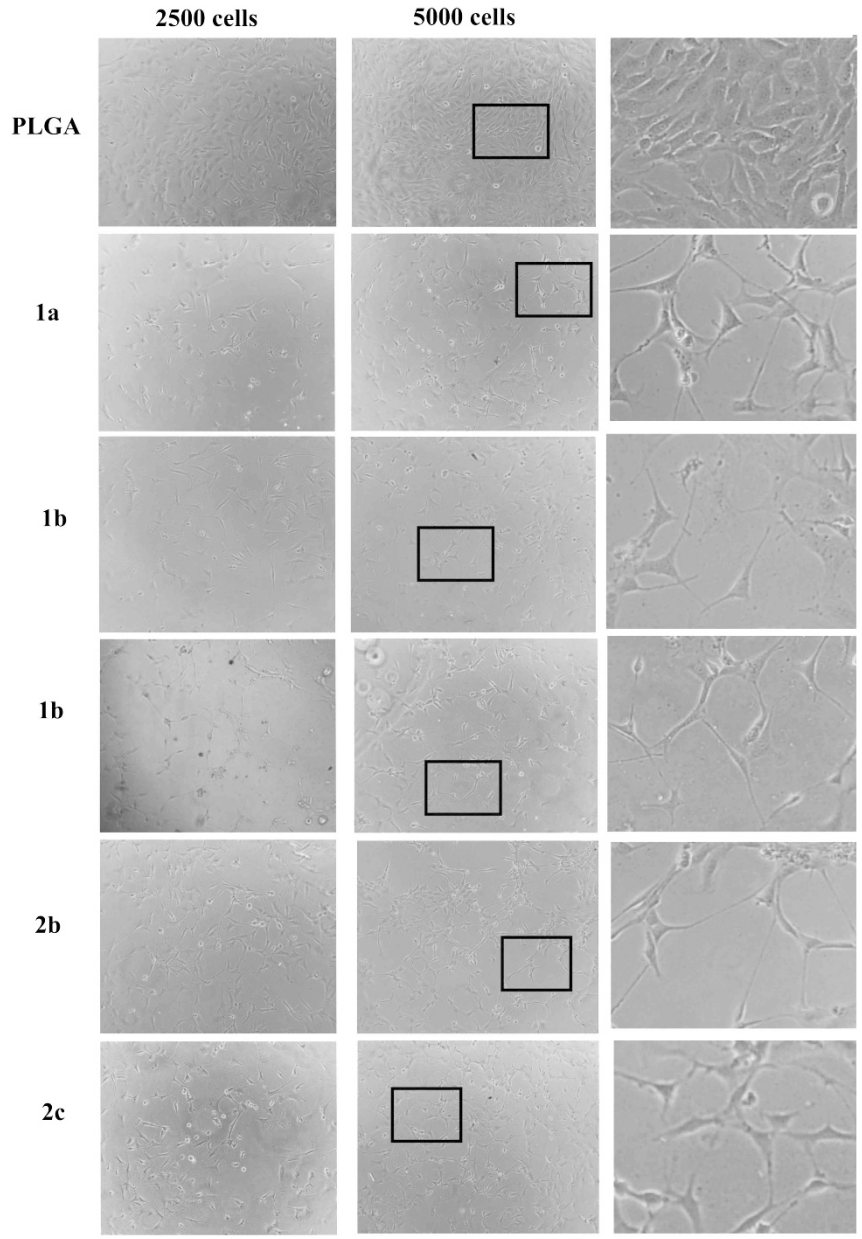

Figure 10 Phase contrast images of *in vitro* cell adhesion after 48 h of culturing by seeding 2500 and 5000 cells (×100 magnification). A magnification of 5000 seeded cell micrographs is shown in the column on the right.

difference between swelling indexes of **1a** and **1b** was not observed, for **2a–c** elastomers we found that as ethylene glycol content increased, the swelling index decreased. These results complement previous observations suggesting that an increase of free OH groups should produce a higher contact angle that hinders water interactions and lowers the swelling index.

Degradation profiles for all elastomers were performed in PBS (pH 7.4) as shown in Figure 7. Over the first 60 days of incubation, mass loss values of 31% and 15% were obtained for **1a** and **1b**, respectively. The lower content of free OH groups and the higher crosslinking degree of **1b** might explain these results. The copolymerization of PGA with ethylene glycol generated a set of elastomers **2a–c** presenting lower degradation rates relative to those of **1a**. These results are likely attributable to the higher hydrophobicity of elastomers **2a–c**. The ethylene glycol-to-glycerol ratio also affected the degradation profiles. Although no significant difference was observed between elastomers **2a** and **2b**, polymer **2c** showed a higher rate of degradation and likely due to its lower crosslinking value.

The mechanical properties of 3- and 5-day-cured elastomers were evaluated. The stress–strain curves of elastomers **1a** and **b** and **2a–c** are presented in Figure 8 and the results obtained from these curves are summarized in Table 3. The glycerol-to-adipic acid ratio of **1a** and **1b** has a profound effect on elastomer YM values. Polymer **1b**, which has the lowest glycerol content, is more rigid and less deformable than **1a**. However, diol incorporation translates into more flexible films with YM values of 1.18 ± 0.18, 0.43 ± 0.01 and 0.07 ± 0.02 MPa for 3-day-cured **2a**, **2b** and **2c**, respectively. In addition, the highest maximum deformation value was obtained for 3-day-cured **2c** with a value of $193.8 \pm 6.1\%$. These results can be attributed to the lowest glycerol/ethylene glycol ratio and hence to the lowest crosslinking level.

Crosslinking values and mechanical properties can also be tailored by modifying curing conditions; thus, the longer the curing period is, the higher the crosslinking degree is due to the formation of new ester bonds. In this way, mechanical properties can be tuned based on variations in curing conditions and monomer ratios to obtain YM values ranging from 0.07 to 8.33 MPa. Within this range, a number of YM values of soft tissues can be included (e.g., nerve tissue (0.45 MPa),[17] cartilage (5.45 MPa),[18] and skin (7.7 MPa))[19].

In vitro cell attachment, proliferation and cytotoxicity

Embryonic mouse fibroblasts (NIH/3T3) were used for *in vitro* cytotoxicity assays of the 5-day-cured polymers. Six hours after seeding, virtually all cells were attached to the **1a** and **b** and **2a–c** elastomeric films with no floating cells observed, as was the case for the cells seeded on plastic (data not shown). However, as is shown in Figure 9a, cells were not able to proliferate in the same manner as those seeded on tissue culture plastic. Moreover, no significant differences were found among the elastomers. To investigate whether there was a cytotoxic effect on the NIH/3T3 cells, fibroblasts were harvested and counted via the trypan blue exclusion method (Figure 9b). High levels of variability were obtained and no significant differences were found among the samples (including all polymers and cells grown on plastic (control)), showing that the elastomers had no detectable cytotoxic effect.

Given that fibroblast NIH/3T3 are pluripotent, cell morphologies were evaluated to identify other types of cells that could result from any differentiation process. Phase contrast images show that fibroblasts underwent a differentiation process (Figure 10). These results explain why cells were not able to proliferate as expected while preserving high levels of viability. Fibroblasts seeded on elastomeric films no longer showed the characteristic elongated morphology exhibited by the positive control. A dendritic morphology as a neuron-like cell type was identified as is shown on micrographic magnifications corresponding to 5000-cell-seeded elastomers shown in the right-hand column of Figure 10.

It is known that physical microenvironments can have a profound effect on the proliferation and differentiation of neural stem cells[20–22] and that the differentiation rate decreases as the YM of surrounding material increases. The YM can affect cell proliferation and can regulate cell type differentiation. It should also be noted that most studies have only investigated the effects of high-YM materials with contradictory results.[23,24] Hence, at this point, we cannot ensure that YM values of such materials are the only factors that regulate the differentiation of NIH/3T3 cells. However, as no differentiation mediators were added to the culture, it is likely that the YM of elastomers have a central role in cell differentiation. Further studies on this type of soft material are needed to develop a stronger understanding of how microenvironments affect cell scaffold interaction outcomes.

CONCLUSION

In the present work, we have prepared a set of biocompatible poly (glycerol adipate)s and poly((glycerol adipate)-*co*-ethylene glycol)s by bulk polymerization. Prepolymers were cured, and the resulting elastomers exhibited promising properties that render them suitable for tissue engineering applications. We note that the final elastomeric properties can be tailored to specific needs by modifying monomer ratios and curing conditions. Cytotoxicity assays were performed on mouse fibroblasts NIH/3T3, and the corresponding results show that cells were able to attach to polymeric films and that they differentiated into neuron-like cell types, highlighting their potential use as scaffolding materials for soft tissue engineering.

CONFLICT OF INTEREST

The authors declare no conflict of interest.

ACKNOWLEDGEMENTS

We would like to acknowledge Prof Dr Santiago Vaillard for his professional assistance with the NMR spectroscopy procedures. We would also like to acknowledge the Consejo Nacional de Investigaciones Científicas y Técnicas (CONICET-Argentina) for its financial support of the present project.

1 Sundback, C. A., Shyu, J. Y., Wang, Y., Faquin, W. C., Langer, R. S., Vacanti, J. P. & Hadlock, T. A. Biocompatibility analysis of poly (glycerol sebacate) as a nerve guide material. *Biomaterials* **26**, 5454–5464 (2005).
2 Göpferich, A. Mechanisms of polymer degradation and erosion. *Biomoterials* **17**, 103–114 (1996).
3 Kemppainen, J. M. & Hollister, S. J. Tailoring the mechanical properties of 3D-designed poly (glycerol sebacate) scaffolds for cartilage applications. *J. Biomed. Mater. Res. A* **94**, 9–18 (2010).
4 Chen, Q.-Z., Bismarck, A., Hansen, U., Junaid, S., Tran, M. Q., Harding, S. E., Ali, N. N. & Boccaccini, A. R. Characterisation of a soft elastomer poly (glycerol sebacate) designed to match the mechanical properties of myocardial tissue. *Biomaterials* **29**, 47–57 (2008).
5 Motlagh, D., Yang, J., Lui, K. Y., Webb, A. R. & Ameer, G. A. Hemocompatibility evaluation of poly (glycerol-sebacate) *in vitro* for vascular tissue engineering. *Biomaterials* **27**, 4315–4324 (2006).
6 Ravichandran, R., Venugopal, J. R., Sundarrajan, S., Mukherjee, S., Sridhar, R. & Ramakrishna, S. Minimally invasive injectable short nanofibers of poly (glycerol sebacate) for cardiac tissue engineering. *Nanotechnology* **23**, 385102 (2012).
7 Li, Y., Cook, W. D., Moorhoff, C., Huang, W. C. & Chen, Q. Z. Synthesis, characterization and properties of biocompatible poly (glycerol sebacate) pre-polymer and gel. *Polym. Int.* **62**, 534–547 (2013).
8 Jeong, S. I., Kim, S. H., Kim, Y. H., Jung, Y., Kwon, J. H., Kim, B.-S. & Lee, Y. M. Manufacture of elastic biodegradable PLCL scaffolds for mechano-active vascular tissue engineering. *J. Biomater. Sci. Polym. Ed.* **15**, 645–660 (2004).
9 Younes, H., Bravo-Grimaldo, E. & Amsden, B. G. Synthesis, characterization and *in vitro* degradation of a biodegradable elastomer. *Biomaterials* **25**, 5261–5269 (2004).
10 Guan, J., Sacks, M. S., Beckman, E. J. & Wagner, W. R. Biodegradable poly (ether ester urethane) urea elastomers based on poly (ether ester) triblock copolymers and putrescine: synthesis, characterization and cytocompatibility. *Biomaterials* **25**, 85–96 (2004).
11 Yang, J., Webb, A. R., Pickerill, S. J., Hageman, G. & Ameer, G. A. Synthesis and evaluation of poly (diol citrate) biodegradable elastomers. *Biomaterials* **27**, 1889–1898 (2006).
12 Zhang, T., Howell, B. A., Dumitrascu, A., Martin, S. J. & Smith, P. B. Synthesis and characterization of glycerol-adipic acid hyperbranched polyesters. *Polymer* **55**, 5065–5072 (2014).
13 Zhang, T., Howell, B. A. & Smith, P. B. Thermal degradation of glycerol/adipic acid hyperbranched poly (ester) s containing either hydroxyl or carboxyl end-groups. *J. Therm. Anal. Calorim.* **122**, 1221–1229 (2015).
14 Taresco, V., Creasey, R., Kennon, J., Mantovani, G., Alexander, C., Burley, J. & Garnett, M. Variation in structure and properties of poly (glycerol adipate) via control of chain branching during enzymatic synthesis. *Polymer* **89**, 41–49 (2016).
15 Kallinteri, P., Higgins, S., Hutcheon, G. A., St. Pourçain, C. B. & Garnett, M. C. Novel functionalized biodegradable polymers for nanoparticle drug delivery systems. *Biomacromolecules* **6**, 1885–1894 (2005).
16 Wyatt, V. T. & Strahan, G. D. Degree of branching in hyperbranched poly (glycerol-*co*-diacid)s synthesized in toluene. *Polymers* **4**, 396–407 (2012).
17 Rydevik, B. L., Kwan, M. K., Myers, R. R., Brown, R. A., Triggs, K. J., Woo, S. L. Y. & Garfin, S. R. An *in vitro* mechanical and histological study of acute stretching on rabbit tibial nerve. *J. Orth. Res.* **8**, 694–701 (1990).
18 Vidal-Lesso, A., Ledesma-Orozco, E., Daza-Benítez, L. & Lesso-Arroyo, R. Mechanical characterization of femoral cartilage under unicompartimental osteoarthritis. *Ing. Mec. Tecnol. Desarro.* **4**, 239–246 (2014).
19 McKee, C. T., Last, J. A., Russell, P. & Murphy, C. J. Indentation versus tensile measurements of Young's modulus for soft biological tissues. *Tissue Eng. Part B* **17**, 155–164 (2011).
20 Engler, A., Sweeney, H., Discher, D. & Schwarzbauer, J. Extracellular matrix elasticity directs stem cell differentiation. *J. Musculoskelet. Neuronal Interact.* **7**, 335 (2007).
21 Engler, A. J., Sen, S., Sweeney, H. L. & Discher, D. E. Matrix elasticity directs stem cell lineage specification. *Cell* **126**, 677–689 (2006).
22 Guilak, F., Cohen, D. M., Estes, B. T., Gimble, J. M., Liedtke, W. & Chen, C. S. Control of stem cell fate by physical interactions with the extracellular matrix. *Cell Stem Cell* **5**, 17–26 (2009).
23 Banerjee, A., Arha, M., Choudhary, S., Ashton, R. S., Bhatia, S. R., Schaffer, D. V. & Kane, R. S. The influence of hydrogel modulus on the proliferation and differentiation of encapsulated neural stem cells. *Biomaterials* **30**, 4695–4699 (2009).
24 Jiang, X. F., Yang, K., Yang, X. Q., Liu, Y. F., Cheng, Y. C., Chen, X. Y. & Tu, Y. Elastic modulus affects the growth and differentiation of neural stem cells. *Neural Regener. Res.* **10**, 1523 (2015).